Electronic Supplementary Material (ESI) for Materials Chemistry Frontiers.

Supplemental Information

An FeS_x Doped Three-Dimensional Covalent Organic Framework for Degradation of Dyes

Jialong Song,[a,b‡] Chengyang Yu,[a‡] Yaozu Liu, [a] Junxia Ren,[a] Jianchuan Liu,[a] Zitao Wang,[a] Liangkui Zhu,[a] Jing Fu,[b] Bin Tang,[c] Shilun Qiu,[a] Yujie Wang*[a] and Qianrong Fang*[a]

Table of contents

Section S1. Materials

S1.1 Materials

All starting materials and solvents, unless otherwise noted, were obtained from J&K scientific LTD and used without further purification. All products were isolated and handled under nitrogen using either glovebox or Schlenk line techniques.

S1.2 Instruments

A Bruker AV-400 NMR spectrometer was applied to record the liquid ^{1}H NMR spectra. Solid-state ^{13}C NMR spectra were recorded on an AVIII 500 MHz solid-state NMR spectrometer. The FTIR spectra (KBr) were obtained using a SHIMADZU IRAffinity-1 Fourier transform infrared spectrophotometer. A SHIMADZU UV-2450 spectrophotometer was used for all absorbance measurements. Thermogravimetric analysis (TGA) was recorded on a SHIMADZU DTG-60 thermal analyzer under N_2. The operational range of the instrument was from 30 °C to 800 °C at a heating rate of 10 °C min^{-1} with N_2 flow rate of 30 mL min^{-1}. PXRD data were collected on a PANalytical B.V. Empyrean powder diffractometer using a Cu Kα source (λ = 1.5418 Å) over the range of 2θ = 2.0−40.0° with a step size of 0.02° and 2 s per step. The sorption isotherm for N_2 was measured by using a Quantachrome Autosorb-IQ analyzer with ultra-high-purity gas (99.999% purity). To estimate pore size distributions for JUC-598, nonlocal density functional theory (NLDFT) was applied to analyze the N_2 isotherm based on the model of N_2@77K on carbon with slit pores and the method of non-negative regularization. For scanning electron microscopy (SEM) image, JEOL JSM-6700 scanning electron microscope was applied. Transmission electron microscopy (TEM) image was obtained on JEM-2100 transmission electron microscopy. The metal loading was determined using inductively coupled plasma (ICP) analyses on a PerkinElmer Optima 3300 DV ICP instrument.

S1.3 Synthesis of 2,3,6,7,14,15-hexa(3-fluoro-4-formylphenyl)triterpene ~~2,3,6,7,14,15-hexa(4′-formylphenyl)triptycene~~ (HFPTP-F)[1]

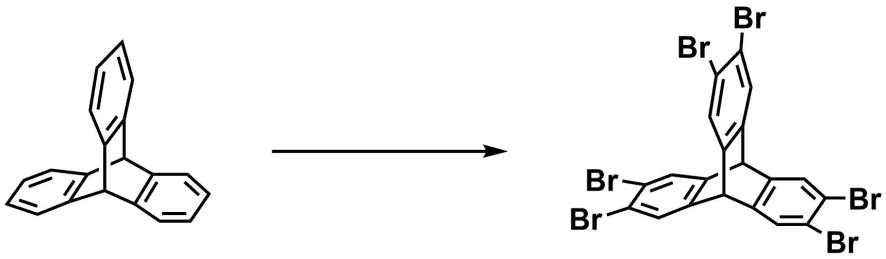

(1) Synthesis of 2,3,6,7,14,15- hexabromotriptycene

A mixture of triptycene (1.00 g, 3.9 mmol) and iron powder (80.0 mg, 1.45 mmol) was dissolved in 1,2-dichloroethane (60.0 mL). Bromine (1.32 mL, 25.7 mmol) was added slowly to the flask. Then the mixture was refluxed for 6h. After the reaction was cooled to 25 °C, the solvent and excess bromine were removed under reduced pressure. The residue was loaded on a short column (silica, CHCl3) to give solid, which was recrystallized from CHCl3 to give the pure product as colorless, needle-like crystals: (2.24 g, 3.1 mmol, 79%), m.p. > 350 °C; ^{1}H NMR (400 MHz, CDCl3, 300 K): δ (ppm) 7.62 (s, 6 H), 5.24 (s, 2 H).

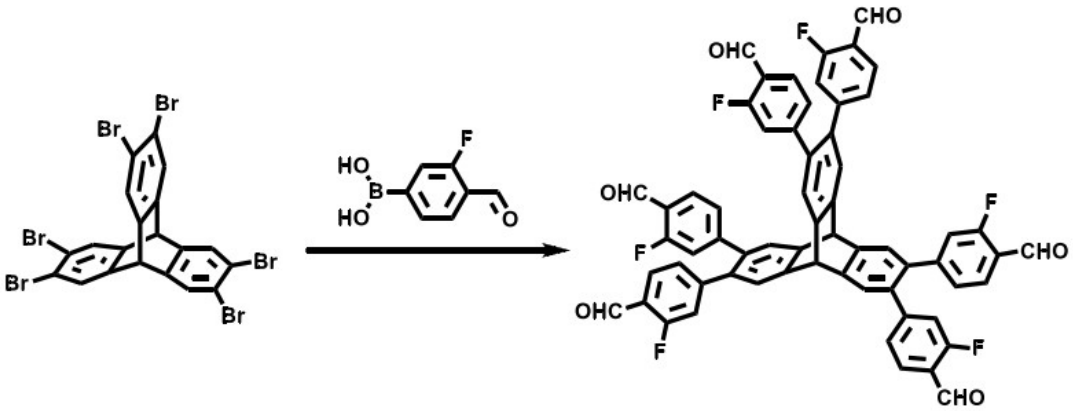

(2) Synthesis of HFPTP-F

A mixture of 2,3,6,7,14,15-hexabromotriptycene (500.0 mg, 0.69 mmol), Cs_2CO_3 (2.90 g, 8.9 mmol.), $Pd(PPh_3)_4$ (0.24 g, 0.2 mmol) and (3-F-4-formylphenyl) boronic acid (1.49 g, 8.9 mmol) was dissolved in anhydrous THF (50.0 mL) and the mixture was heated and stirred at 65 °C under an argon atmosphere for 18 h. The solvent was removed under reduced pressure and the residue was dissolved in CH_2Cl_2 (100.0 mL). The crude product was washed sequentially with saturated $NaHCO_3$ (100.0 mL), deionized H_2O (100.0 mL), and brine (100.0 mL). The organic phase was dried with $MgSO_4$ and filtered. The solvent was removed in vacuo and the crude product was

purified by column chromatography with silica gel (CH_2Cl_2/methanol, 50:1, v/v) and gave the pure product as yellow-white crystals (364 mg, 0.37 mmol, 53 %), m.p. >300 °C. 1HNMR (400 MHz, ^{1}HNMR (400 MHz, $CDCl_3$)：δ (ppm) = 10.30 (s, 6 H), 7.71-7.74 (m, J = 7.88, 6 H), 7.60 (s，6 H), 6.90-6.97 (m, J = 8.04, 12 H), 5.76 (s, 2 H). ^{13}C NMR (100 MHz, $CDCl_3$-*d*6, δ)：δ (ppm) = 186.659, 165.533, 162.952, 148.977, 148.891, 144.883, 136.136, 128.772, 126.294, 122.823, 122.742, 117.773, 117.561, 52.913.

S1.4 Synthesis of 1,3,6,8-tetra(4-aminophenyl)pyrene (TAPPy)[2]

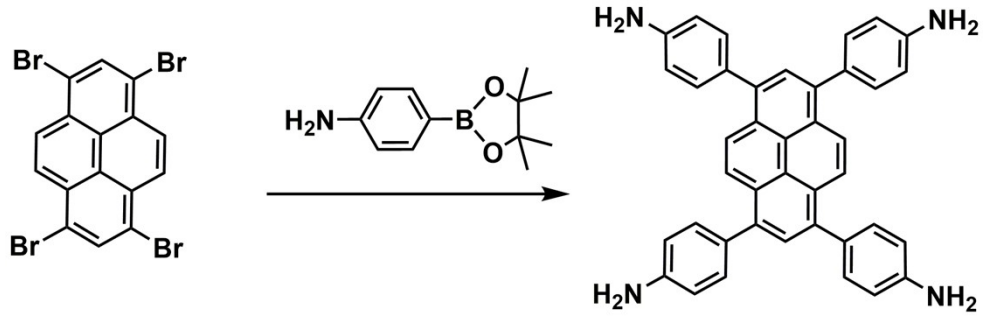

A mixture of 1,3,6,8-tetrabromopyrene (1.48 g, 2.86 mmol), 4-aminophenylboronic acid pinacol ester (3.01 g, 13.7 mmol), K_2CO_3 (2.18 g, 15.7 mmol), and $Pd(PPh_3)_4$ (0.33 g, 0.29 mmol, 10 mol%) was dissolved in 32.0 mL 1,4-dioxane and 8.0 mL degassed H_2O and the mixture was heated and stirred at 115 °C under an argon atmosphere for 3 d. After cooling to room temperature, H_2O (50.0 mL) was added. The resulting precipitate was collected via filtration and was washed with H_2O (50.0 mL) and MeOH (100.0 mL). Recrystallization from 1,4-dioxane, followed by drying under high vacuum furnished the title compound, as a bright yellow powder (1.69 g, 2.56 mmol, 89 %). ^{1}H NMR (400 MHz, $CDCl_3$) δ (ppm): 8.13 (s, 4 H), 7.79 (s, 2 H), 7.34 (d, *J* = 8.4 Hz, 8 H), 6.77 (d, *J* = 8.5 Hz, 8 H), 5.30 (s, 8 H), 3.56 (s, 12 H, dioxane).^{13}C NMR (400 MHz, $CDCl_3$) δ: 148.2, 137.1, 131.0, 129.0, 127.6, 126.7, 126.1, 124.4, 113.9, 66.3 ppm.

Section S2. Characterization

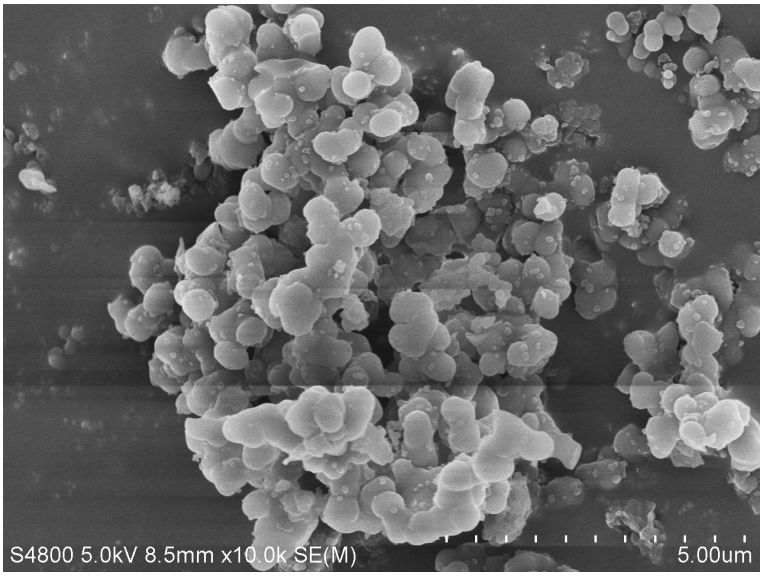

Figure S1. SEM image of as-synthesized JUC-598.

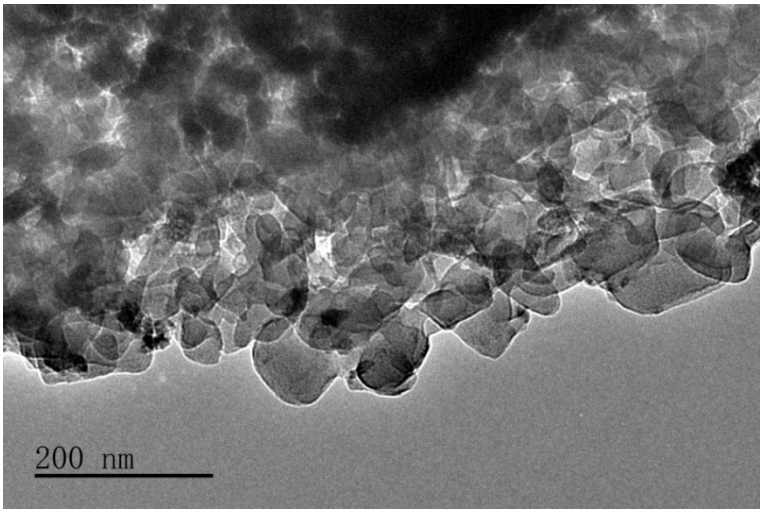

Figure S2. TEM image of as-synthesized JUC-598.

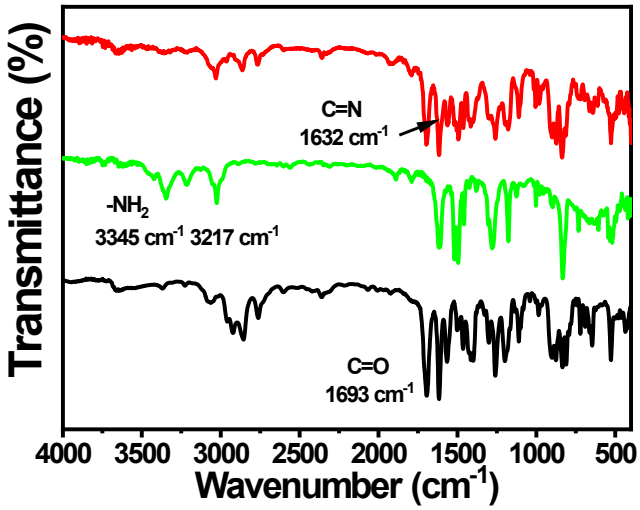

Figure S3. FT-IR spectra of HFPTP-F (black) and TAPPy (green), JUC-598 (red).

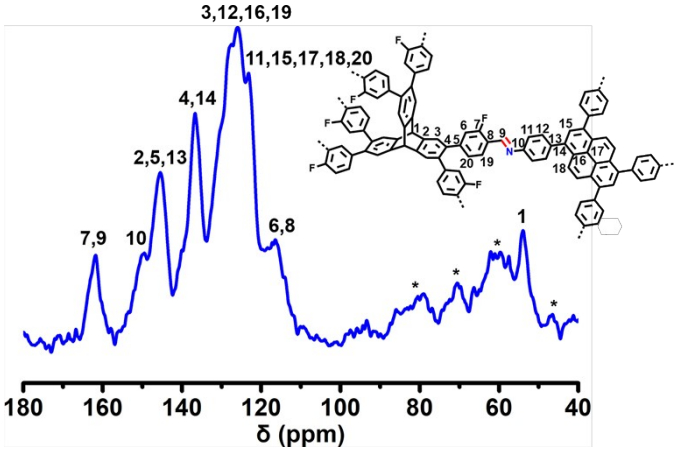

Figure S4. Solid state ^{13}C NMR of JUC-598. Asterisks (*) indicate peaks arising from spinning side bands.

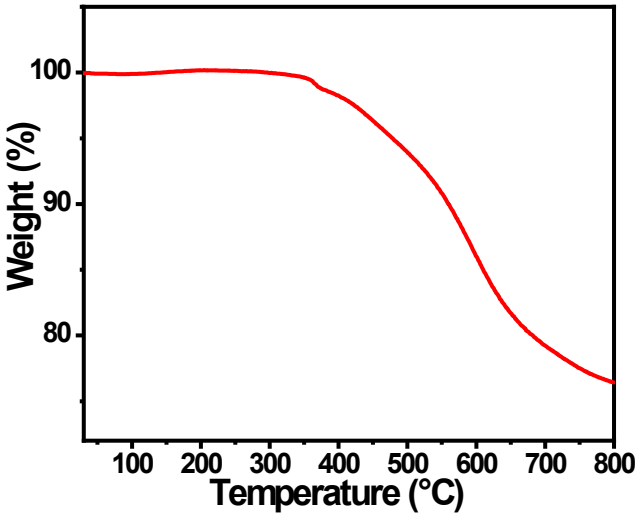

Figure S5. TGA curve of JUC-598.

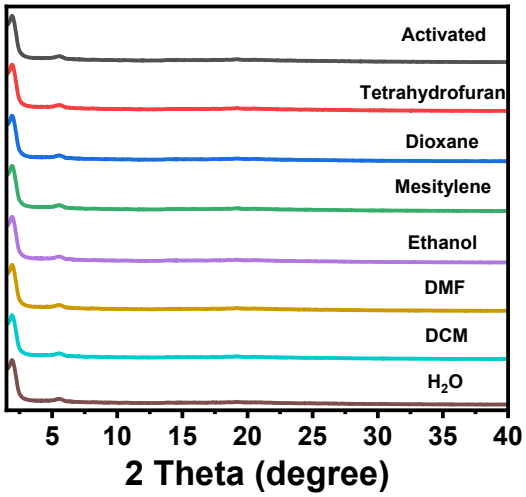

Figure S6. A comparison of PXRD patterns of JUC-598 before and after the activation and treatment in various organic solvents and water for 24 h.

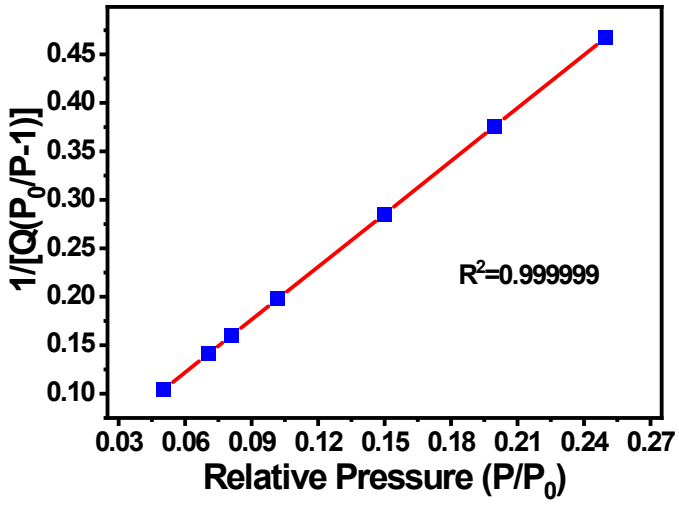

Figure S7. BET plot of JUC-598 calculated from N_2 adsorption isotherm at 77 K.

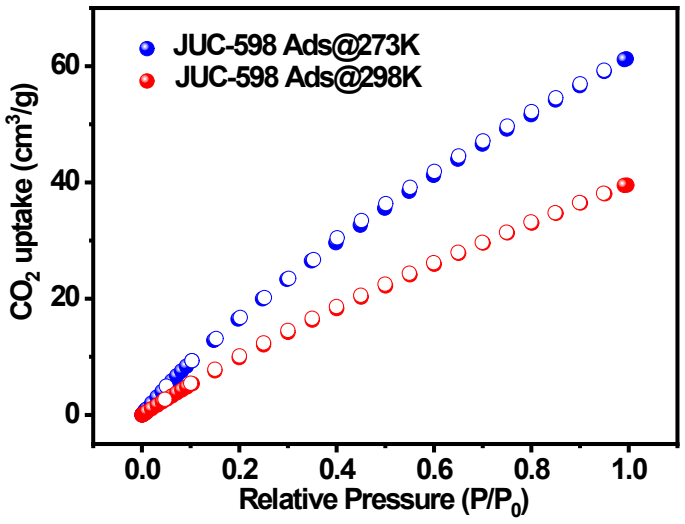

Figure S8. CO_2 adsorption of JUC-598 at 77 K and 87 K.

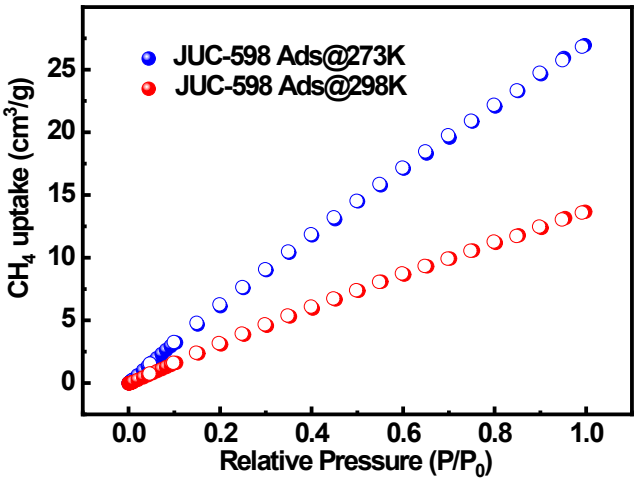

Figure S9. CH_4 adsorption of JUC-598 at 77 K and 87 K.

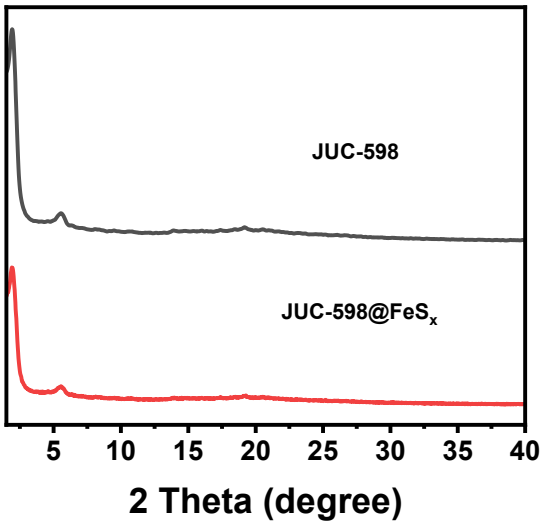

Figure S10. PXRD patterns of JUC-598 and JUC-598@FeS_x.

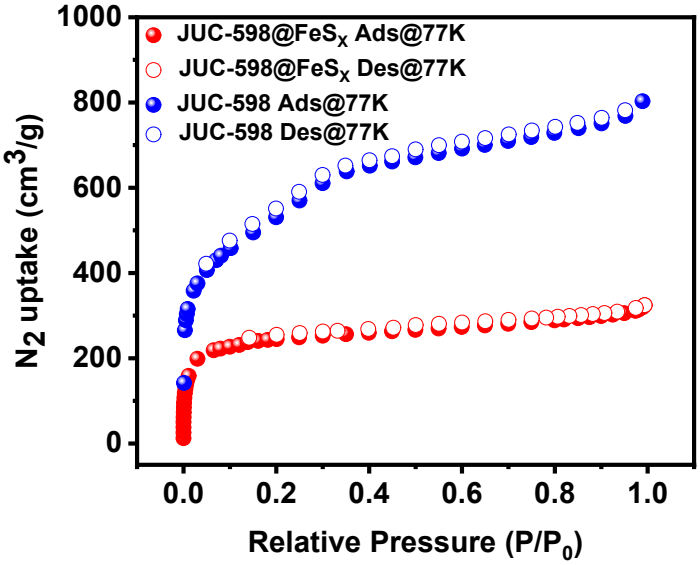

Figure S11. N_2 adsorption-desorption isotherm of JUC-598 and JUC-598@FeS_x at 77 K.

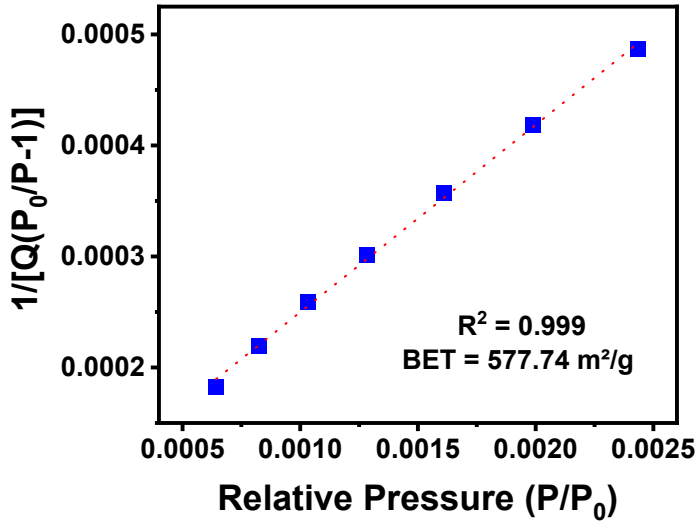

Figure S12. BET plot of JUC-598@FeS_x calculated from N_2 adsorption isotherm at 77 K.

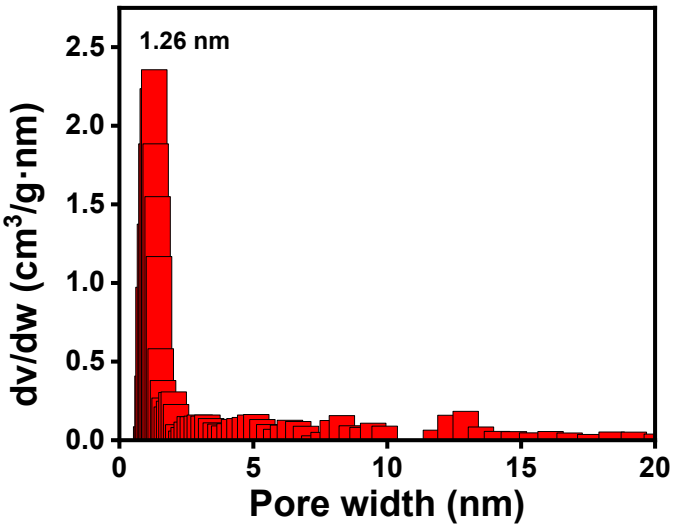

Figure S13. The pore-size distribution of JUC-598@FeS_x indicating a microporous width of ~1.2 nm

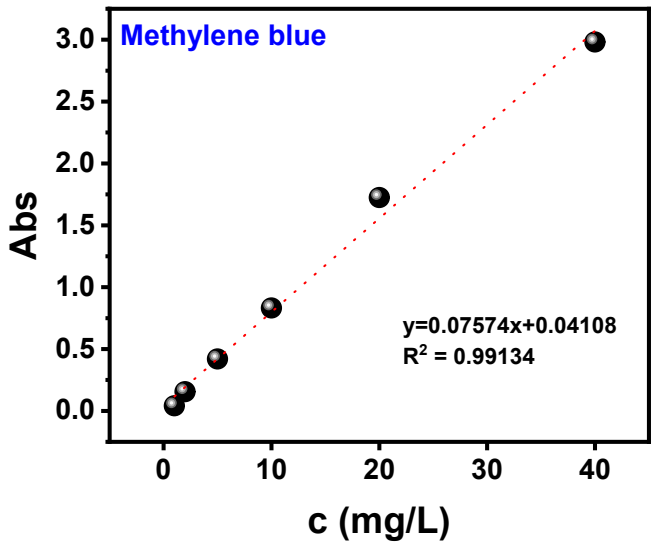

Figure S14. The standard UV-vis curve of MB.

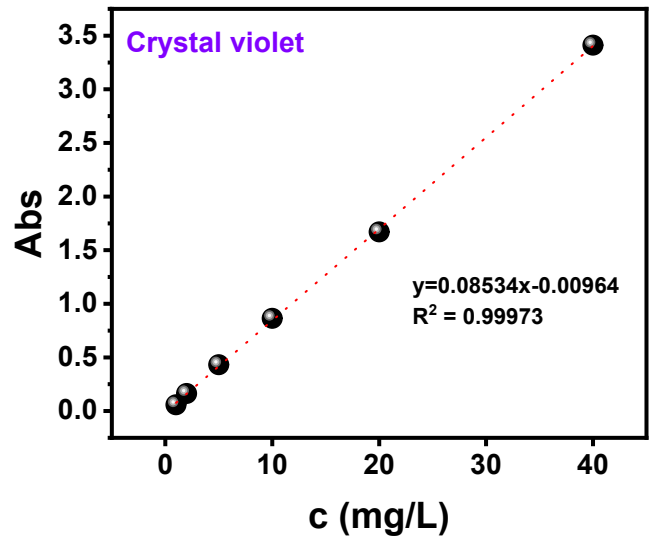

Figure S15. The standard UV-vis curve of CV.

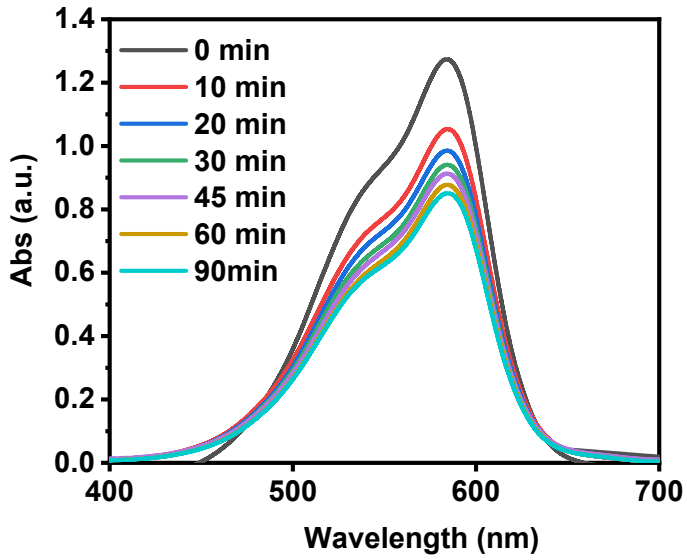

Figure S16. Evolution of UV-vis absorption spectra of CV solution (15 mg/L) in the presence of JUC-598 (adsorption capacity of 32.71%)

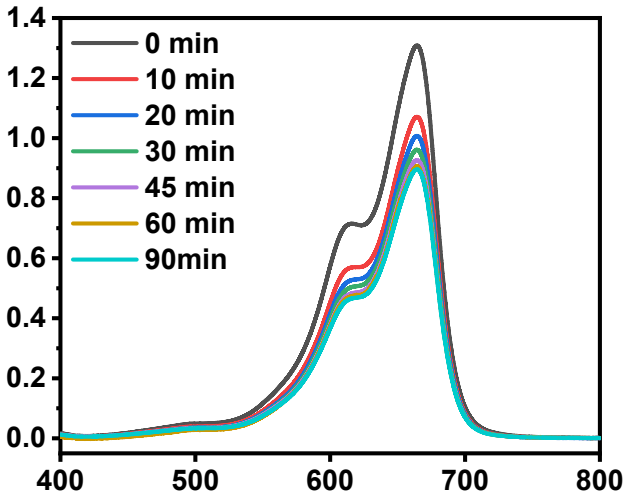

Figure S17. Evolution of UV-vis absorption spectra of MB solution (15 mg/L) in the presence of JUC-598 (adsorption capacity of 32.47%)

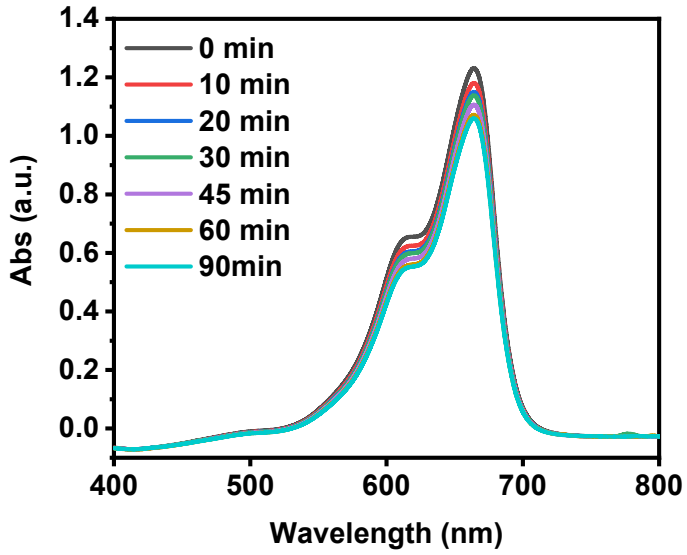

Figure S18. Evolution of UV-vis absorption spectra of MB solution (15 mg/L) in the presence of JUC-598@FeS_x.

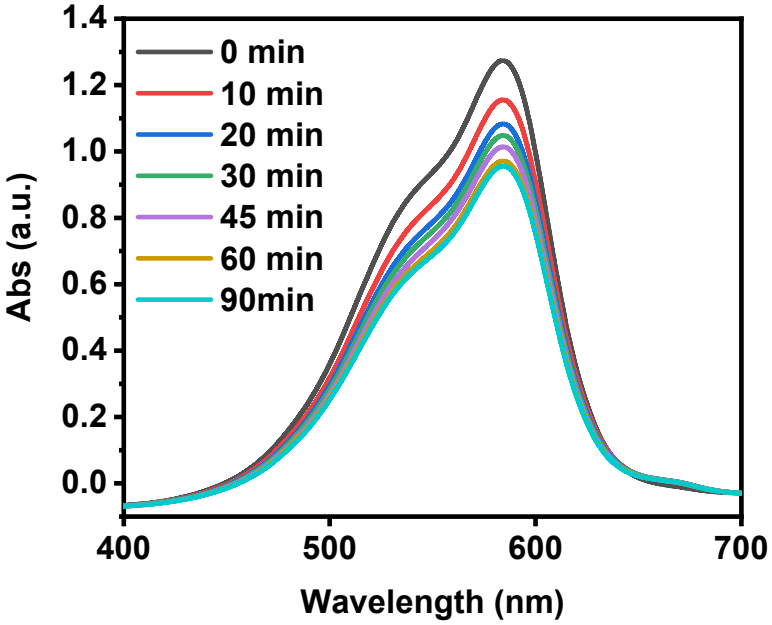

Figure S19. Evolution of UV-vis absorption spectra of CV solution (15 mg/L) in the presence of JUC-598@FeS_x

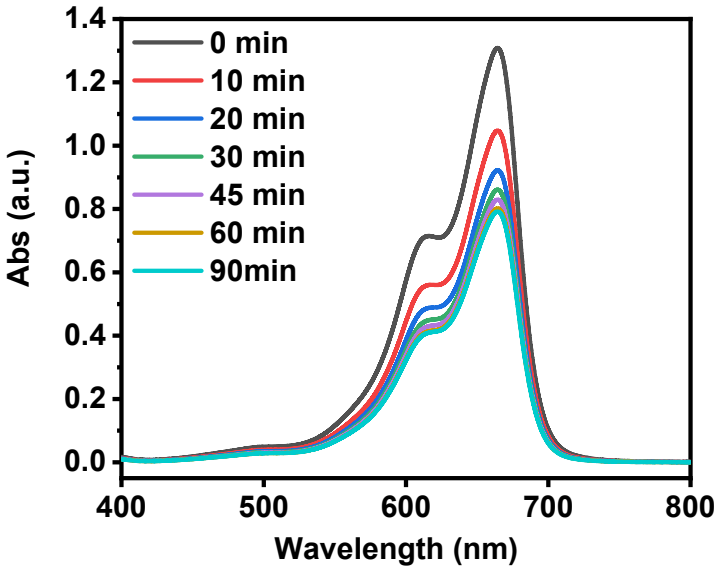

Figure S20. Evolution of UV-vis absorption spectra of MB solution (15 mg/L) in the presence of FeS_x (degradation capacity of 38.9%)

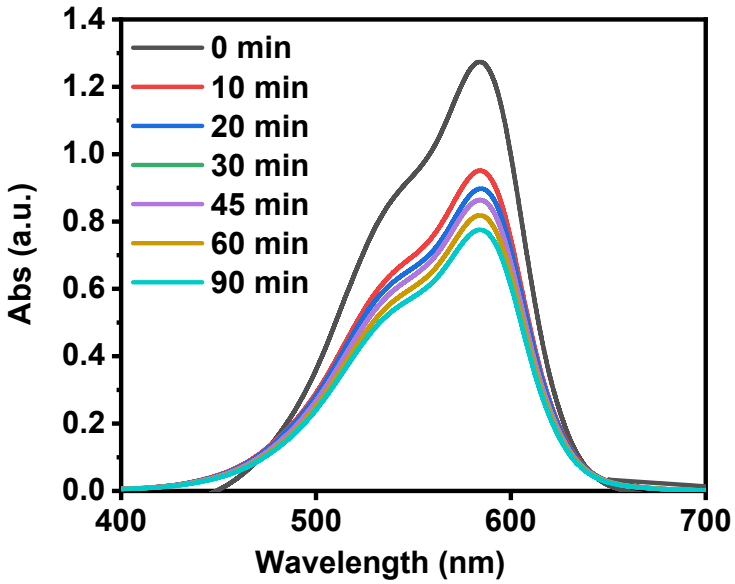

Figure S21. Evolution of UV-vis absorption spectra of CV solution (15 mg/L) in the presence of FeS_x (degradation capacity of 40.4%)

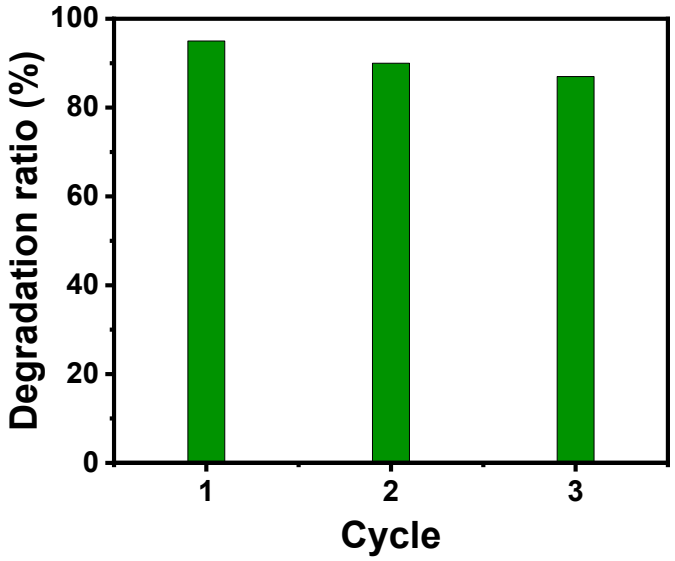

Figure S22. Recyclability study of JUC-598@FeS_x for CV.

.

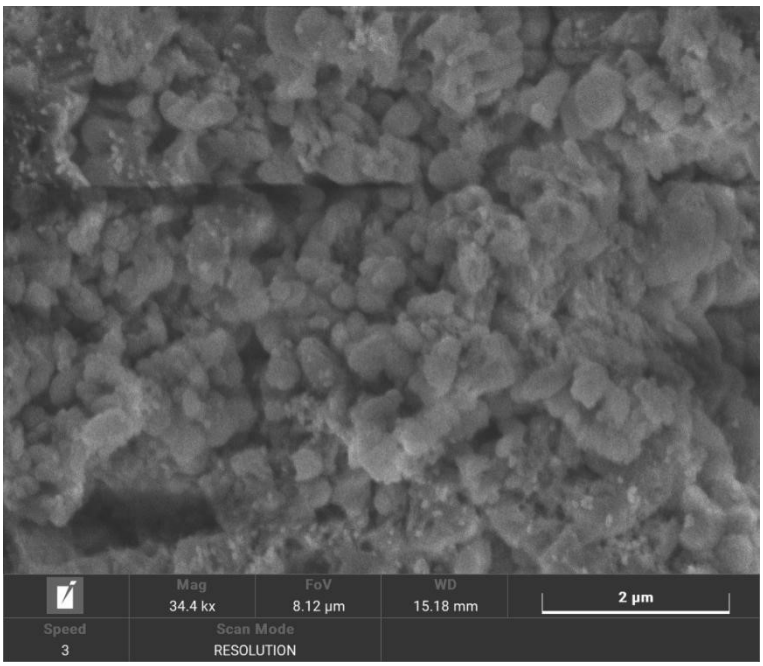

Figure S23. The SEM of JUC-598@FeS_x after Fenton reaction.

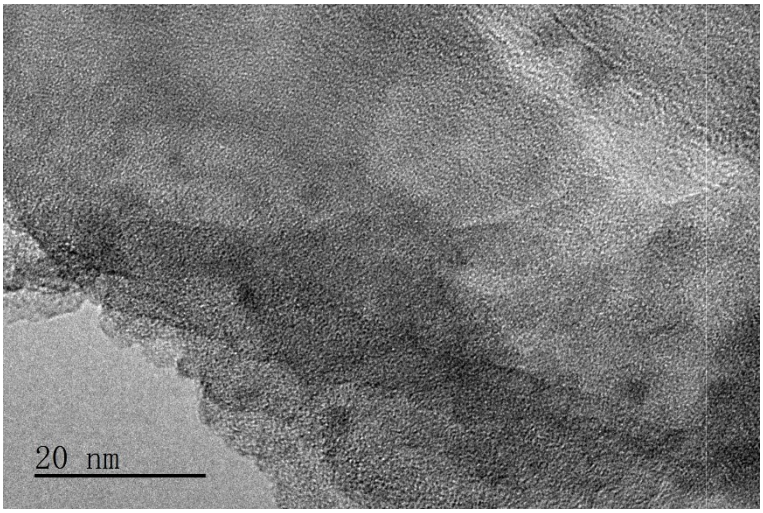

Figure S24. The TEM of JUC-598@FeS_x after Fenton reaction.

Table S1. Unit cell parameters and fractional atomic coordinates for JUC-598 calculated based on the **stp** net.

Space group	*P6/m*		
Calculated unit cell	$a = b = 53.5268$ Å，$c = 19.9307$ Å，$\alpha = \beta = 90°$，$\gamma = 120°$		
Measured unit cell	$a = b = 53.5126$ Å，$c = 19.9218$ Å，$\alpha = \beta = 90°$，$\gamma = 120°$		
Pawley refinement	$R_p = 2.52\%$，$R_{wp} = 3.26\%$		
atoms	x	y	z
C1	0.4011	0.6261	0.5738
C2	0.4307	0.6441	0.5844
C3	0.4464	0.6339	0.6198
C4	0.4326	0.6056	0.6454
C5	0.4027	0.5878	0.6347
C6	0.3871	0.5980	0.5992
C7	0.4493	0.5951	0.6829
N8	0.4367	0.5694	0.7088
C9	0.4329	0.5317	0.7837
C10	0.4504	0.5565	0.7461
C11	0.4804	0.5675	0.7451
C12	0.4925	0.5540	0.7823
C13	0.4749	0.5296	0.8211
C14	0.4450	0.5183	0.8210
C15	0.4881	0.5157	0.9282
C16	0.4878	0.5153	0.8603
C17	0.3846	0.6367	0.5356
C18	0.3682	0.6462	0.5710
C19	0.4775	0.5323	0.9667

C20	0.3521	0.6557	0.5356
F21	0.4752	0.6518	0.6290
H22	0.4421	0.6671	0.5642
H23	0.3912	0.5648	0.6551
H24	0.3630	0.5833	0.5910
H25	0.4736	0.6097	0.6894
H26	0.4085	0.5222	0.7841
H27	0.4950	0.5873	0.7137
H28	0.5168	0.5630	0.7813
H29	0.4305	0.4981	0.8516
H30	0.3681	0.6461	0.6282
H31	0.4691	0.5452	0.9390
C32	0.5000	0.5000	0.8202
C33	0.5000	0.5000	0.0341
H34	0.5000	0.5000	0.7630
C35	0.3333	0.6667	0.4330
H36	0.3333	0.6667	0.3758

Section S3. References

1. C. Moylan, L. Rogers, Y. M. Shaker, M. Davis, H.-G. Eckhardt, R. Eckert, A. A. Ryan and M. O. Senge, Preparation of Tri- and Hexasubstituted Triptycene Synthons by Transition Metal Catalyzed Cross-Coupling Reactions for Post-Modifications, *Eur. J. Or. Chem.*, 2016, **2016**, 185-195.
2. D. Bessinger, L. Ascherl, F. Auras and T. Bein, Spectrally Switchable Photodetection with Near-Infrared-Absorbing Covalent Organic Frameworks, *J. Am. Chem. Soc.*, 2017, **139**, 12035-12042.